

Temperature and Grain Size Effect on the Electrical Conductivity of $La_{0.67}Ca_{0.33}MnO_3$

Mohammed. I. Mohammed¹, A. A. Elbadawi^{2*}, H.H. Abuellhassan²

¹Department of Physics, Faculty of Education, Nile Valley University, Attbra 11121 Sudan

²Department of Physics, Faculty of Science and Technology, Alneelain University, Khartoum 11121 Sudan

(Received: June 11, 2013; Accepted: August 12, 2013)

Abstract— A study for different samples of the compound of the single Perovskite $La_{0.67}Ca_{0.33}MnO_3$ has been performed as a function of grain size and investigated by X-ray Diffraction (XRD), Scanning Electron Microscopy (SEM) and Electrical Resistivity Measurement Setup (ERMS). It is found that the crystal structure remains the same for all the samples, while the grain size decreases with the increases of the grinding time and it increases with sintering temperature. At the low temperature measurement of resistivity, it is found that the values of the metal-insulator transition temperature T_{MI} depends upon the grain size effect, whereas it decreases with the increases of the grain size. The scattering process appears to be dominated by electron-electron interaction process.

Index Terms— Grain size, Electrical conductivity, X-ray Diffraction (XRD), Scanning Electron Microscopy (SEM), Electrical Resistivity Measurement Setup (ERMS)

I. INTRODUCTION

In the early fifties Jonker and Van Santen (1950) reported on the preparation of polycrystalline mixed-valence manganites [1]. They discussed the structural and magnetic properties $La_{1-x}A_xMnO_3$. They found that the manganites crystallize in the perovskite structure and observed a close relationship between the doping factor x and the structural and magnetic properties. They showed that the end-members with $x = 0$ and $x = 1$ are anti-ferromagnetic, while the compositions with $x \approx 0.3$ are ferromagnetic. Zener suggested an explanation for this phenomenon, introducing the so-called double exchange mechanism a ferromagnetic exchange coupling between magnetic ions in different valence states [2]. Volger measured the magnetoresistance, i.e. the change of resistance due to application of a magnetic field, of a sintered ceramic $La_{0.8}Sr_{0.2}MnO_3$ [3]. He observed a negative magnetoresistance of about 8 % near the Curie temperature of the compound. In the nineties new interest in mixed-valence manganites was prompted by the discovery of very large magnetoresistance values in high-quality thin films. Jin reported on thousand-fold change in resistivity and a corresponding magnetoresistance of 127,000 % in a La-Ca-

Mn-O thin film (at 77 K and with an external field of 6 T) [4]. They called this effect colossal magnetoresistance (CMR). The CMR effect has also been observed for Sr- and Ba-doped lanthanum manganites [5].

Today, the mixed-valence manganites are very generally termed CMR materials, although the extremely large magnetoresistance values are found only in high-quality thin films.

II. MATERIALS AND METHODS

Lanthanum manganites (and manganites in general) can be prepared by many different synthesis techniques and in various forms, including single crystals, polycrystalline ceramics and thick or thin films. Single crystals can be grown in several ways, for instance by the floating-zone method [1]. Polycrystalline samples can be prepared by solid state mixing (which was used here), involving repeated steps of mixing, grinding and heating of oxides until a single-phase manganite is obtained. Polycrystalline manganites can also be synthesized by various wet-chemical methods [6]. Thick manganite films can be produced by spraying techniques and well-defined 2D-patterns can be obtained using screen printing techniques [7]. Thin films are usually grown by laser ablation (pulsed laser deposition) or sputtering using sintered polycrystalline targets [8]. Depending on the substrate, thin films can be prepared in epitaxial as well as polycrystalline forms [9].

Raw materials La_2O_3 , $CaCO_3$ and MnO_2 of purity more than 99.9% were used for preparing the sample of weight 6 grams, are calculated using the equation:



These amounts are added together and hand grinded continuously in the presence of acetone for homogeneity. After drying the sample was put in a crucible and allowed to undergo solid state reaction by calcinations in a furnace at 950 °C for 8 hrs. This step (calcinations) was repeated for twice to remove the carbonates from the sample. After cooling gradually inside the furnace to room temperature, the sample was grinded thoroughly and divided into 2 parts (A and B) each part is 3 grams. Then the A was divided into 3 parts, every part is 1gram.

The first 1g was left without grinding, the second was grinded for 3 hrs and the third for 6 hrs, using the ball milling machine. And these three samples were pressed into rectangular plates and then sintered to about 9hrs at the furnace in 1100 °C.

These steps were done also in part B but with 1300°C sintering.

Then these samples were analyzed by XRD, SEM at room temperature and the resistance has been measured as a function of temperature down to $T \approx 40\text{K}$.

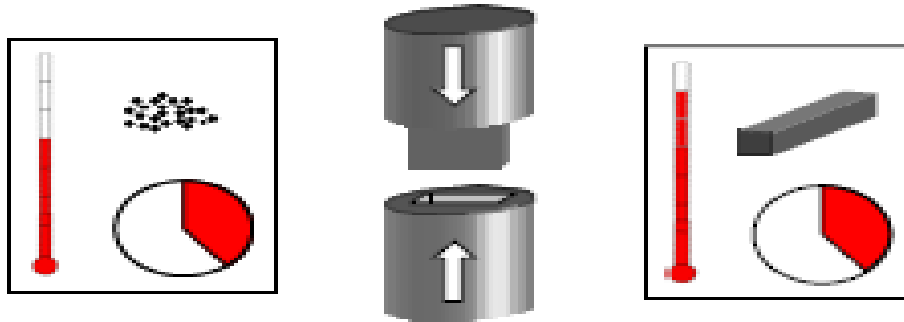


Fig: (1) Steps of solid state reaction preparation method (calcinations in air at 950 °C, powder pressing and sintering in air at 1100 °C and 1300 °C for 9 hrs).

III. RESULTS AND DISCUSSION

1. The X-ray Diffraction Result (XRD)

Three perovskite manganite samples of $\text{La}_{0.67}\text{Ca}_{0.33}\text{MnO}_3$ were prepared at different conditions that named here as A, B and C respectively, have been studied by x-ray diffraction (XRD) at room temperature.

The x-ray of the samples have been indexed and found to be orthorhombic and single phase without any detectable secondary phases **Figure 2**.

The intensity of x-ray peaks for the samples is increased as the sintering temperature increases. Also the intensity increases as the grain size increases which indicates that the crystalline of the samples become better with higher sintering temperature. **Table (1)** summarizes the preparation conditions.

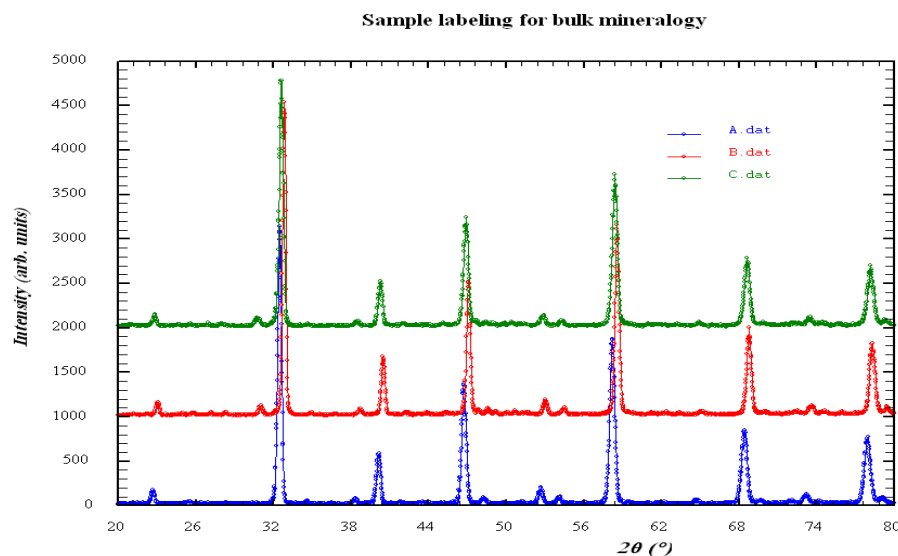


Fig: (2) the x-ray pattern for the three samples.

Table (1)

The variation of intensity in three samples sintered at temperature 1300 C⁰

Sample	Milling time (hours)	Intensity (arb. units)
A	0	3168
D	3	3181
E	6	3564

Figure (1) has been taken to compare the three samples .It is noticed that there is an additional peak at 31⁰ which was seen in the XRD data for the both samples B and C where it doesn't present in sample A.

It is cleared from **Fig (3)** that as the sintering temperature increases there is a decreasing in the full width at half maximum (FWHM) and hence the crystallite size is inferred to increase as in **figure (3)** below:-

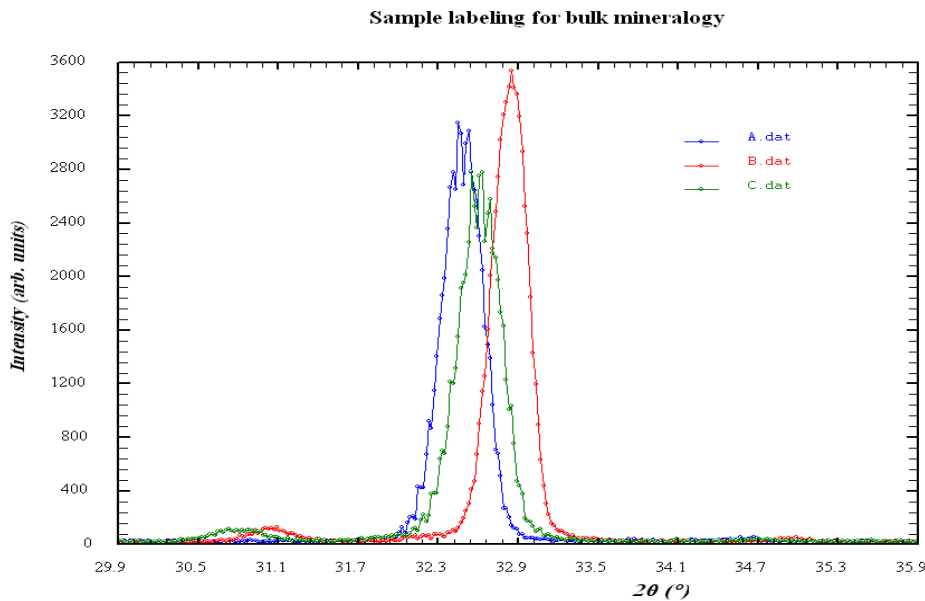


Fig: (3) the x-ray pattern for the three samples from 29.90 to 35.90.

There was a small shift in the peak position due to the effect of the grinding time.

Table (2)

The variation of the intensity in the three samples

Sample	Ts(C ⁰)	Milling time (hours)	Intensity (arb units)
A	1300	0	3168
B	1300	6	3564
C	1100	6	2802

The average crystallite sizes (ACS) of grain are obtained from x-ray line width using Scherer formula:

$$ACS = k\lambda / \beta \cos \theta \quad (1)$$

Where: $k \approx 0.89$ the factor shape.

λ : Wavelength of x-rays,

β : The difference in width of the half maximum of the peak

θ : The angle of diffraction.

The ACS of the samples A, B and C obtained are found to be 23 nm, 21 nm and 16nm, respectively. Which it decreases with grinding time and increases with sintering temperature.

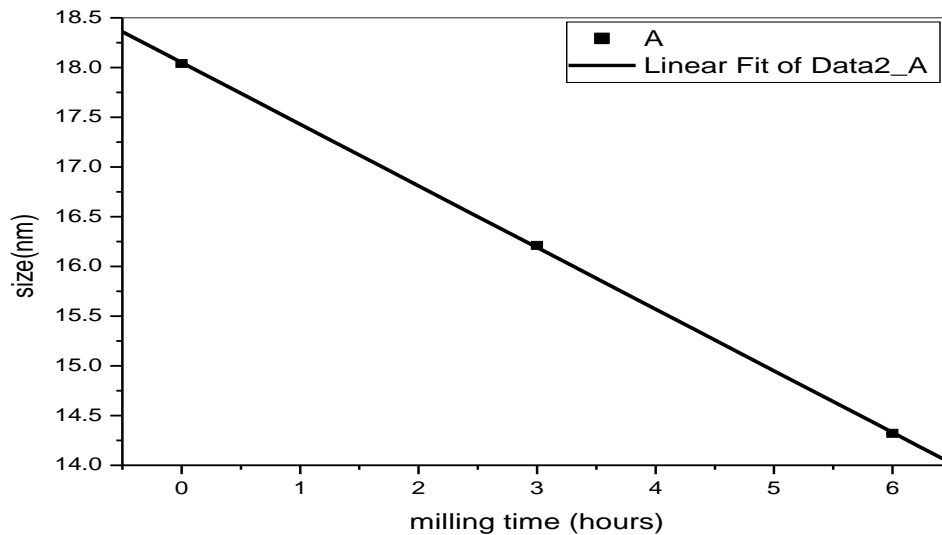


Fig: (4) the relation between the average crystallite size, sintering temperature and milling time, respectively.

The effect of grinding can be noticed in the fig (4) where as shown see the average crystallite size is decreased with the time of grinding increases.

Table (3)

The size variation of the three samples

Sample	T _s (C ⁰)	Milling time (hours)	Size (nm)
A	1300	0	18.04
D	1300	3	16.21
E	1300	6	14.32

2. Result of Scanning Electron Microscopy (SEM)

The grain size and surface morphology of the three samples A, B and C were investigated by using Scanning Electron Microscopy (SEM) of the same size. Figures (5, 6 and 7) show the results of SEM of the samples, respectively. It is noticed that in figure (5) the grains are compacted (closed together) and mostly regular in shape whereas in figure (6) there is a space from the ground,

this space was seen in figure (7) but with less brightness than (6), because of sintering.

In fig (6) and fig (7) the SEM micrographs were shown for the samples B and C, respectively. These samples were undergone ball-milling for 6 hours and sintered at 1300C⁰ and 1100C⁰.

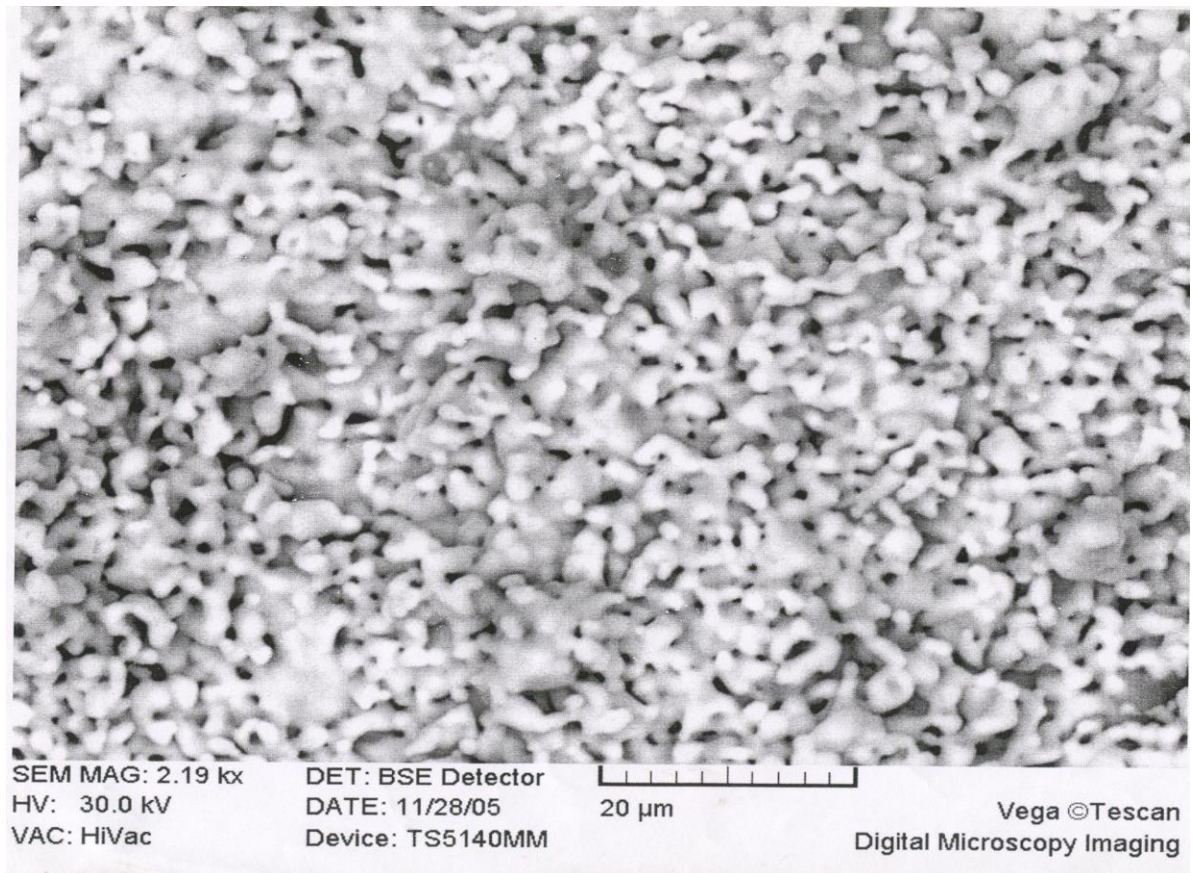


Fig: (5) the image of SEM for sample A (0 hours grinding and 1300C⁰ sintered)

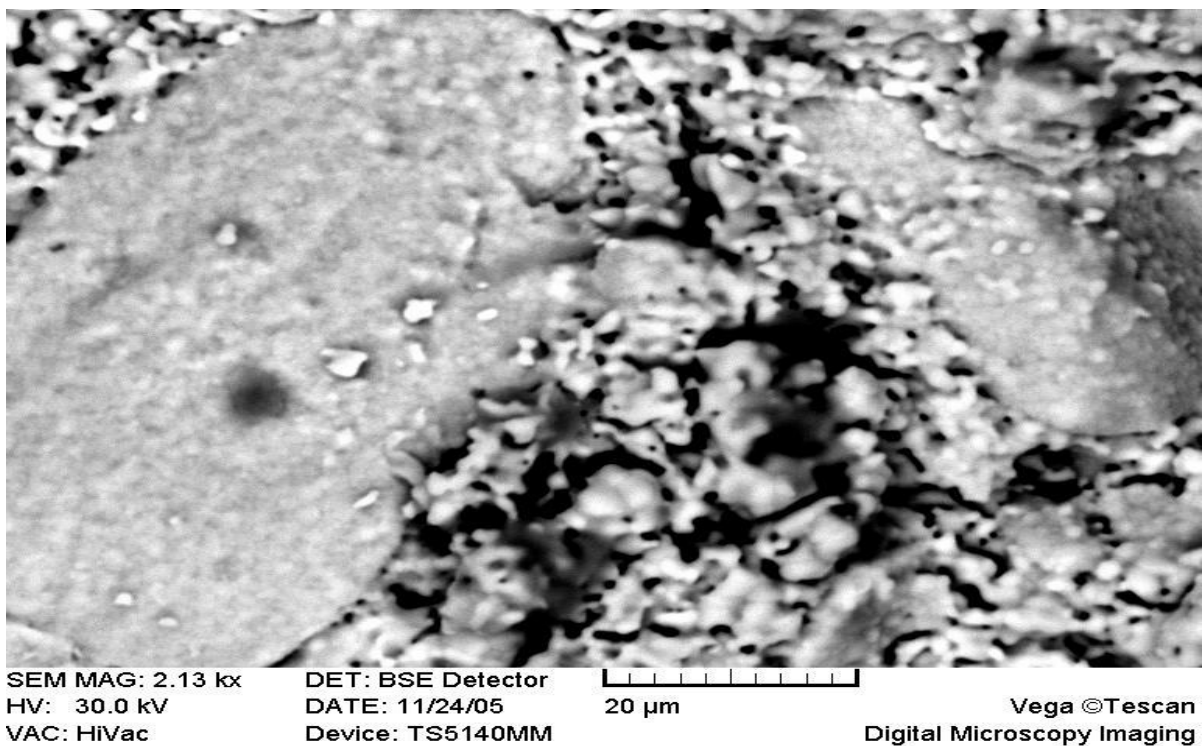


Fig: (6) the image of SEM for sample B (6 hours grinding and 1300C⁰ sintered)

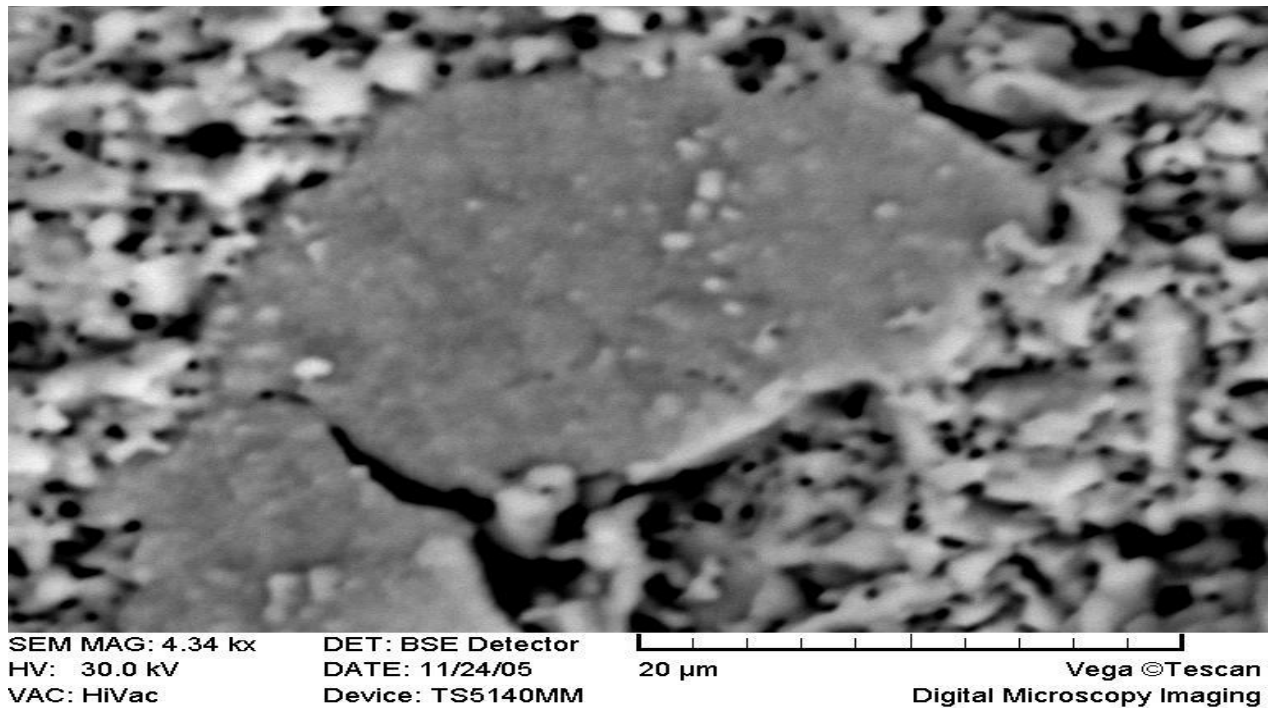


Fig: (7) the image of SEM for sample C (6 hours grinding and 1100C⁰ sintered)

The observation reveals that there is a distribution of particle size, poor particle connectivity and high porosity in sample B and C, whereas sample A has a well connected particle and a less porosity than sample B and C.

3. Results and Analysis of the Electrical Resistivity

It is noted that the maximum peak of the resistivity shifts with low temperature, increases with the grinding time and decreases with the sintering temperature.

The relationship between $\rho(T)$ and T for the three samples was shown in figure (8). The peak resistivity value of sample A is 1692.10 (ohm.cm), it is the lowest because there was no grinding, the resistivity value of sample B is 528.238 (ohm.cm) which is higher than A

because of the grinding, and the resistivity value of sample C 136.023 (ohm.cm) is the highest one.

There is a transition temperature T_C of the three samples A, B and C which is 212.6K, 185.4K and 175.2K respectively. These values were determined and plotting against T.

Finding $d\rho/dT$ versus T, in this curve it is noticed that $T_{MI} = 176.066K, 188.006K$ and $213.519K$ for the samples A, B and C respectively.

Table (4)

The variation of T_{MI} in the three samples

Sample	$T_s(C^0)$	Milling time (hours)	$T_{MI}(K)$
A	1300	0	176.066
B	1300	6	188.006
C	1100	6	213.519

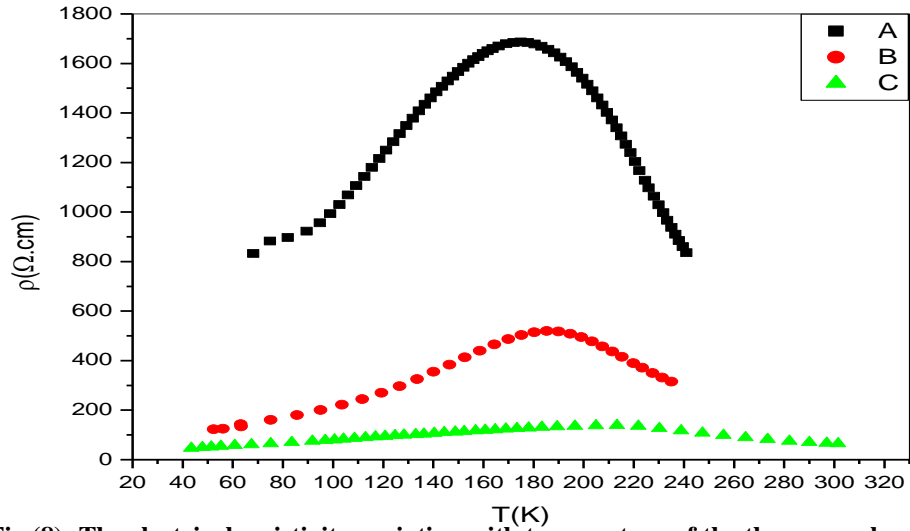


Fig (8): The electrical resistivity variation with temperature of the three samples.

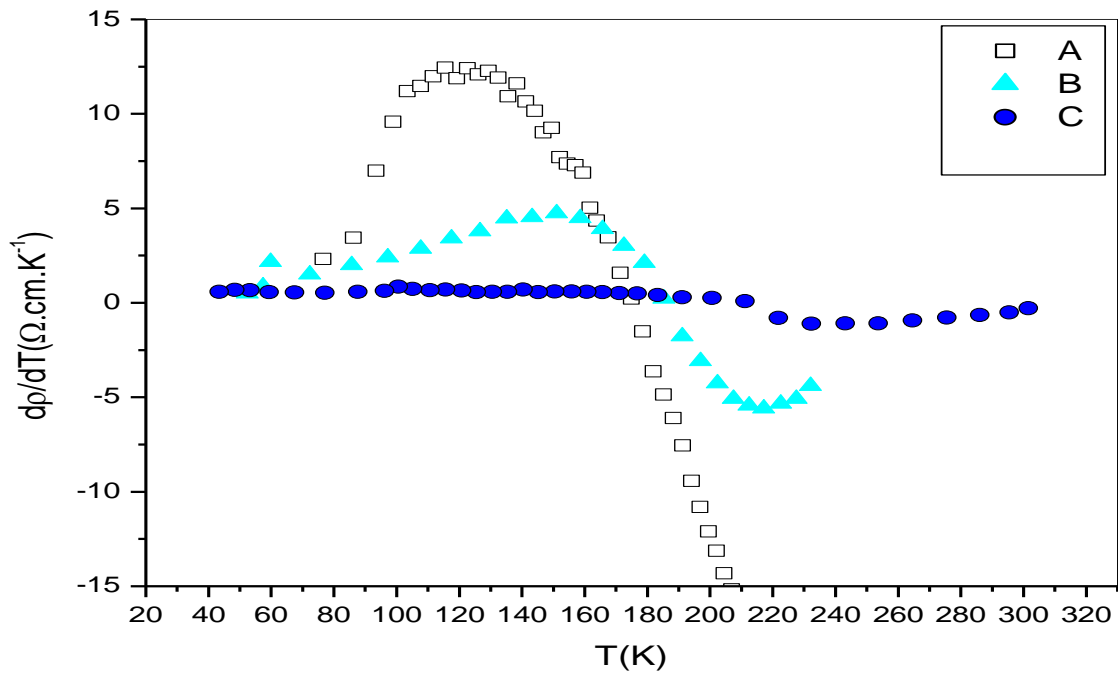


Fig: (9) $d\rho/dT$ Vs T for the three samples.

Figure (9) was used to determine the metal-insulator transition temperature T_{MI} . T_{MI} is the temperature at which $d\rho/dT = 0$.

In perovskite manganites the presence of electron-electron interaction ($\rho \propto T^2$), the scattering electron by single Magnon ($\rho \propto T^{2.5}$) and the scattering of electrons by two Magnons ($\rho \propto T^{4.5}$) had been proposed [10].

The following equation can be used to interpret the plot of variation of electrical resistivity with temperature

$$\rho(T) = \rho_o + AT^2 + BT^{4.5} \quad (2)$$

Or,

$$\rho(T) = \rho_o + CT^{2.5} \quad (3)$$

Where: ρ_o represents the residual resistivity for A, B and C are the constants.

Plotting of $\rho(T)$ Vs T^2 , $T^{2.5}$ and $T^{4.5}$ are made to the data plotting below T_c . These plotting are shown in figures (10, 11 and 12).

The values of the constant A, B, C and ρ_o are shown in tables (9, 10 and 11)

It has been recognized that fig (10), the fitting line is mostly linear in the temperature range $10000K^2 - 20000K^2$, $5000K^2 - 32500K^2$ and $2500K^2 - 40000K^2$ for the three samples, respectively.

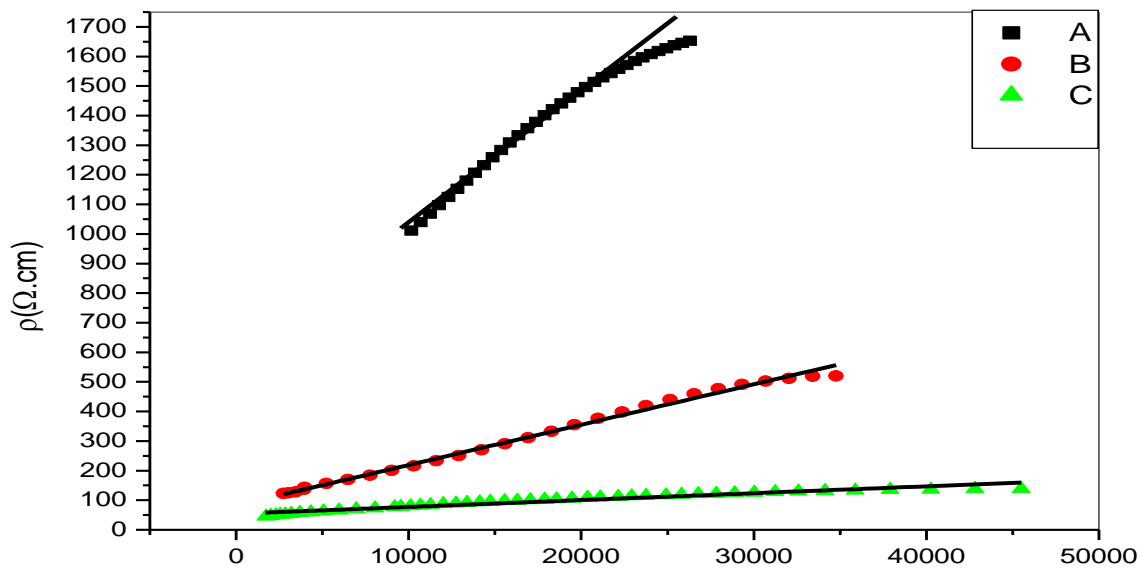


Fig: (10) the variation of the resistivity as T^2 for the three samples.

Table (5)

The variation of resistivity in the three samples at T^2 .

Sample	ρ_o	$\rho_2 (\Omega.cm.K^{-2})$
A	637.57	0.041
B	82.61	0.013
C	54.20	0.002

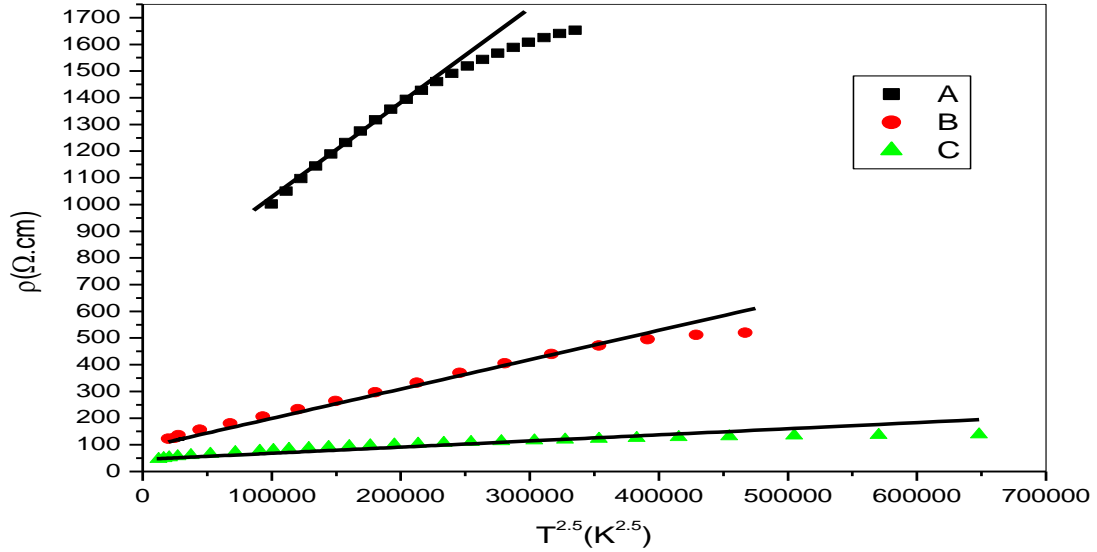


Fig: (11) the variation of the resistivity as $T^{2.5}$ for the three samples.

Table (6)

The variation of resistivity in the three samples at $T^{2.5}$

Sample	ρ_0	$\rho_{2.5} (\Omega.cm.K^{-2.5})$
A	761.47	0.0029
B	88.93	0.0011
C	45.30	0.0002

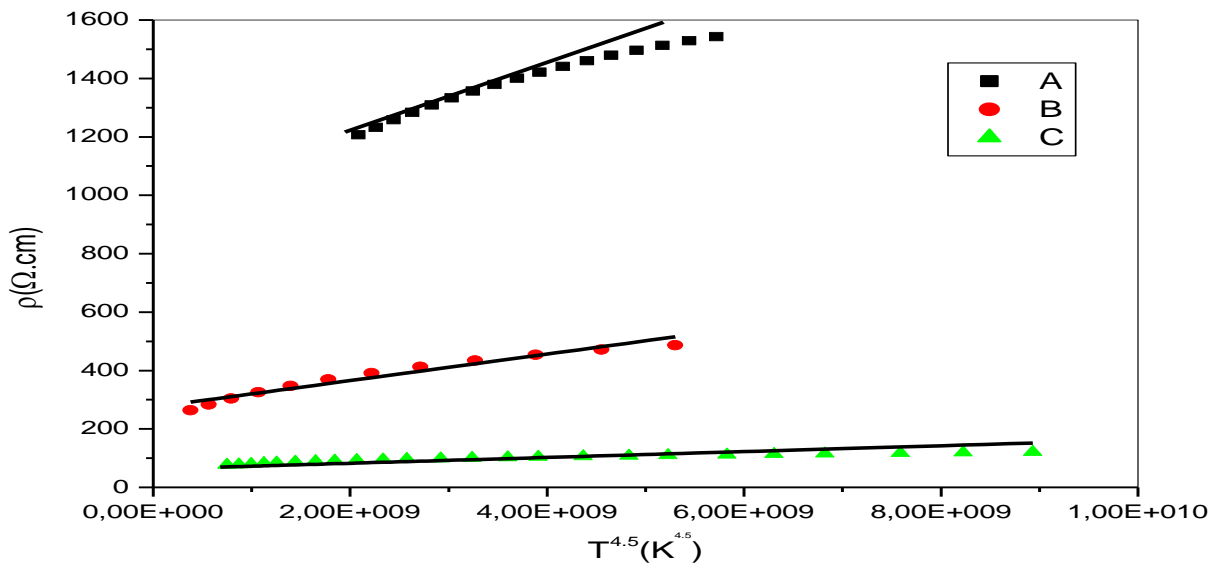


Fig: (12) the variation of the resistivity as T^2 for the three samples.

Table (7)
The variation of resistivity in the three samples at T^{4.5}.

Sample	ρ_0	$\rho_{4.5} (\Omega.cm.K^{-4.5})$
A	1048.08	9.17E-8
B	274.59	4.45E-8
C	62.52	1E-8

From these tables it is found that the value of the coefficient ρ_2 is significantly large than the other scattering process [11].

4. Discussion and conclusion

$La_{0.67}Ca_{0.33}MnO_3$ Polycrystalline samples have been prepared under different sintering temperature and mechanical grinding time.

The samples were investigated by X-ray Diffraction (XRD), scanning Electron Microscopy (SEM) and Electrical Resistivity Measurement (ERM) as a function of temperature. The grain size was found to decrease with sintering at low temperature and grinding for long time. These finding was supported by (SEM) images.

The intensity of the x-ray peaks for the samples increases as the sintering temperature increases indicating that the crystalline becomes better with higher sintering temperature [12]. It is obvious from the peaks that as the sintering temperature increases there is a decrease in the full width at half maximum (FWHM) and hence the crystalline size increases.

The temperature dependence of electrical resistivity showed a clear variation in its behavior, which signifies that the grain size effect plays an important roles in the electrical transport properties of the manganites, Zhu et.al [13]. Who had studied the grain size effect on the electrical properties of $La_{0.8}Ca_{0.2}MnO_3$. They found that the value of the low temperature resistivity of the samples increases with decreasing grain size. Our results are in good agreement with these reported data.

For the majority spin electrons the temperature dependence of the resistivity due to the electron-electron scattering would provide the T² dependence, however the T² term is about 60 times larger than the expected one for this type of scattering. Typical values of the residual resistivity ρ_0 are less than $4 \times 10^{-3} \Omega cm$ which can be considered a check of high quality of the samples. Even grain of the order $10 \mu m$ has strong effect on both ρ_0 and $\rho(T)$ at low temperatures [14].

The low temperature metallic property of the electrical resistivity shows that the scattering process that governs the conduction process is sensitive to the grain size effect.

Throughout the temperature range of the measurement, there is a significant contribution from the electron-electron interaction process to the conduction mechanism in this type of manganites.

The values of the coefficient differ from each other, which decreases with grain size decrease or time grinding increases.

Finally we conclude that the grain size affects in the conductivity of the manganites at low temperature. It is demonstrated that the smaller grain size results in a low electrical conductivity.

REFERENCES

- [1] Jonker GH, Van Santen JH. Ferromagnetic compounds of manganese with perovskite structure. Physica. march (1950) **16** (3), 337–349.
- [2] Zener C. Interaction between the d shells in the transition metals. Physical Re-view (1951a) **81** (4), 440–444.
- [3] Volger J. Further experimental investigations on some ferromagnetic oxidic compounds of manganese with perovskite structure. Physica. (1950) **20**, 49–66.
- [4] Jin S, McCormack M, Tiefel TH, and Ramesh R. Colossal magnetoresistance in La-Ca-Mn-O ferromagnetic thin films. Journal of Applied Physics. (1994) **76** (10), 6929–6933.
- [5] Von Helmolt R, Wecker J, Haupt L, and Bärner K. Intrinsic giant magnetore-sistance of mixed valence La-A-Mn oxide (A = Ca, Sr, Ba). Journal of Applied Physics. (1994) **76** (10), 6925–6928.
- [6] Goldschmidt V. Geochemistry. Oxford University Press. (1958).
- [7] Shannon RD. Revised effective ionic radii and systematic studies of intera-tomic distances in halides and chalcogenides. Acta Crystallographica. (1976) **A32** (5), 751–767.
- [8] Coey JM, Viret DM, and Ranno L. Electron localization in mixed-valence manganites. Physical Review Letters. (1995) **75** (21), 3910–3913.
- [9] Nagaev EL. Lanthanum manganites and other giant magnetoresistance mag-netic conductors. Physics – Uspekhi. (1996) **39** (8), 781–805.
- [10] Zhou T Z, Zhong YW, Xu XN, Zhang HH, and Du YW. Larger magne-tocaloric effect in two-layered $La_{1.6}Ca_{1.4}Mn_2O_7$. Journal of Applied Physics. (1999) **85** (11), 7975–7977.

- [11] Shannon RD. Revised effective ionic radii and systematic studies of interatomic distances in halides and chalcogenides. *Acta Crystallographica*. (1976) **A 32** (5), 751–767.
- [12] Liu Changshi, Prediction of the Magneto-Resistance of $\text{La}_{0.67}\text{Ca}_{0.33}\text{MnO}_3$ and $\text{La}_{0.8}\text{Sr}_{0.2}\text{MnO}_3$ via Temperature and a Magnetic Field. *J. Chem. Eng. Data*, (2011), **56** (1), 2–8.
- [13] Zhu T, Sun JR. and Shen BG. Grain-boundary effects on the electrical resistivity and the ferromagnetic transition temperature of $\text{La}_{0.8}\text{Ca}_{0.2}\text{MnO}_3$. *Appl. Phys. Lett.* (2000) **77**, 118.
- [14] Ling F, Zhu L, et al. Structure and magnetotransport properties of epitaxial nano composite $\text{La}_{0.67}\text{Ca}_{0.33}\text{MnO}_3$: SrTiO_3 thin films grown by a chemical solution approach. *Appl. Phys. Lett.* (2012) **100**, 082403.